Notes

Contribution from the Laboratories for Inorganic
Materials, Department of Chemistry, Concordia University,
1455 de Maisonneuve Boulevard West,
Montreal, Quebec, Canada H3G 1M8

Solvent Effects and Excited-State Dynamics in Photochemical Ligand Substitution of $W(CO)_5L$ (L = pip, py)

Carol Moralejo and Cooper H. Langford*

Received October 19, 1989

Introduction

The photochemistry of $M(CO)_6$ (M = Cr, Mo, W) and its derivatives has been studied extensively.[1-5] For $M(CO)_6$ (M = Cr, W), photosubstitution reactivity is wavelength independent.[2,3] All photoinitiated substitution reactions appear to proceed via the thermally equilibrated triplet state. In contrast, for $W(CO)_5L$ (L = an N-donor), where loss of L is the predominant reaction with substitution yields ≥ 0.5, the first studies of these systems revealed wavelength dependence.[4,5] For these complexes, substitution can proceed directly from the LF singlet state.[6] In this recent work, two distinct pathways for substitution of L into $W(CO)_5L$ (L = py, pip) were observed: a more efficient pathway from the LF singlet state and a less efficient pathway from the LF triplet state.[6] Quantum yields are lower upon 457.9- and 488-nm irradiations, which directly populate the triplet state (^3E), compared to the quantum yields upon 436-nm irradiation, which populates a combination of LF singlet and LF triplet states. The lowest yields are found upon 488-nm irradiation. The highest yields are observed upon 436-nm irradiation (excitation of the ^1E state). Moreover, wavelength dependence is observed within the LF singlet region, as was first reported by Wrighton,[4] with lower yields associated with irradiation into the ^1A band.

Substitution of the unique ligand occurs following excitation of either the ^1A or the ^1E bands, but substitution is more efficient from the ^1E state. This suggests that efficient crossing between the ^1A and the ^1E states occurs with reaction originating from the ^1E state. Higher yields for irradiation into the ^1E regions than for irradiation into either the ^1A or ^3E regions indicate that processes of reactive relaxation and radiationless decay to the ground state are both competitive with internal conversion and intersystem crossing processes among these excited states. This raises the question of which parameters control state to state crossing and radiationless decay.

Laser flash photolysis has provided evidence for the existence of an intermediate pentacarbonyl species from $M(CO)_6$ (M = Cr, Mo, W) which can interact with a variety of relatively noncoordinating solvents to form $M(CO)_5S$.[7-12] We have found from our recent work[13] that the solvo intermediate, $W(CO)_5S$, is formed from $W(CO)_5L$ (L = pyridine, piperidine) in cyclohexane in less than 10 ps under 355-nm irradiation. Formation of $W(CO)_5S$ from $W(CO)_6$ is slower.[6,13] Recent work reported by Lee and Harris[14] using subpicosecond flash photolysis of $Cr(CO)_6$ in both cyclohexane and THF indicates that vibrational relaxation of the reactive pentacarbonyls to produce ground-state $Cr(CO)_5S$ is controlled by the surrounding solvent.

The present report attempts to elucidate the factors via analysis of solvent effects. It should be noted that since luminescence is negligible, the sum of reaction yield and yield for return to the ground state is 1.

Experimental Section

Materials. Isooctane, dichloromethane, chloroform, and carbon tetrachloride were spectroscopic grade solvents purchased from Aldrich. THF (Aldrich, reagent grade) was distilled over potassium metal before use. Benzene (distilled in glass) was purchased from Caledon. 1-Hexene (99%+) was purchased from Aldrich. $W(CO)_6$ (Aldrich, 99%) was used without further purification. Reaction mixtures were typically prepared by adding *x* mL of 1-hexene to 2*x* mL of unreactive solvent.

$W(CO)_5$py and $W(CO)_5$pip were prepared by a modification of the procedure proposed by Strohmeier.[15] A 0.65-g sample of $W(CO)_6$ was dissolved in 30 mL of THF, and 5 mL of pyridine or piperidine was added. The solution was irradiated by exposure to "cool-white" fluorescent laboratory lights ($\lambda > 350$ nm) for 72 h. Prepurified N_2 was passed through a solvent bubbler to prevent solvent evaporation and into the solution to sweep out displaced CO. The reaction was monitored for unreacted $W(CO)_6$ by TLC on alumina plates. After 72 h, the THF was removed by rotary evaporation. The yellow residue was dissolved in benzene, and the solution was treated with 1-2 g of alumina. The benzene was evaporated overnight to encourage adsorption of the product onto the alumina. The adsorbed product was added to a column of neutral alumina in isooctane. Isooctane first eluted unreacted $W(CO)_6$, and then benzene eluted the product. Ethanol was used to elute the unreacted ligand. The product was recrystallized from benzene/isooctane (1:1). Purity was established by comparison with published UV-vis spectra.[4,5] The yield was greater than 70%.

Irradiation Procedures. Samples were irradiated in a cylindrical fused quartz cell with optically flat windows (Hellma, 1-cm path length, 19-mm diameter, 2.8-mL volume). A PRA Model 3402 medium-pressure Xe arc lamp (150 W), coupled with the appropriate interference filters, was used for photolysis at 313, 365, and 436 nm (±10 nm). All reactions were monitored by UV-visible absorption spectroscopy using a microprocessor-controlled Hewlett Packard Model 8452A diode array spectrophotometer with ±2 nm resolution. Each sample was irradiated for successive time intervals and a full spectrum taken after each irradiation period. Solutions were manually mixed at intervals during each irradiation run and prior to analysis. The amount of light absorbed by the $W(CO)_5L$ reactants was determined on the basis of the light absorbed by the well-known potassium ferrioxalate chemical actinometer.[16] The samples were not degassed prior to irradiation, since previous experiments[6] have shown that there is no difference in reactivity between aerated and deaerated solutions. Data from less than 10% conversion were used for calculation of quantum yields.

Electronic Spectral Band Deconvolution. The electronic spectra of $W(CO)_5L$ (L = py, pip) in all solvents used in this study were deconvoluted by using a Gaussian band least-squares minimization routine developed by Belliveau[17] employing a Marquardt algorithm.[18] The program allows the band positions to be fixed and the best Gaussian fits for the MLCT, and ligand field ^1A and ^1E bands were determined when the positions of the ^3E band maxima were initially fixed.

---

(1) Geoffroy, G. L.; Wrighton, M. *Organometallic Photochemistry*; Academic Press: New York, 1979.
(2) Nasielski, J.; Colas, A. *J. Organomet. Chem.* **1975**, *101*, 215.
(3) Nasielski, J.; Colas, A. *Inorg. Chem.* **1978**, *17*, 237.
(4) Wrighton, M.; Hammond, G. S.; Gray, H. B. *Mol. Photochem.* **1973**, *5*, 179.
(5) Wrighton, M. *Inorg. Chem.* **1974**, *13*, 905.
(6) Moralejo, C.; Langford, C. H.; Sharma, D. K. *Inorg. Chem.* **1989**, *28*, 2205.
(7) Nasielski, J.; Kirsch, P.; Wilputte-Steinert, L. *J. Organomet. Chem.* **1971**, *29*, 269.
(8) Bonneau, R.; Kelly, J. M. *J. Am. Chem. Soc.* **1980**, *102*, 1220.
(9) Lees, A. J.; Adamson, A. W. *Inorg. Chem.* **1981**, *20*, 4381.
(10) Breckenridge, W. H.; Steward, G. M. *J. Am. Chem. Soc.* **1986**, *108*, 364.
(11) Perutz, R. N.; Turner, J. J. *J. Am. Chem. Soc.* **1975**, *97*, 4791.
(12) Tyler, D. R.; Petrylak, D. P. *J. Organomet. Chem.* **1981**, *212*, 389.
(13) Moralejo, C. Ph.D. Thesis, Concordia University, Montreal, 1989; pp 95-97.
(14) Lee, M.; Harris, C. B. *J. Am. Chem. Soc.* **1989**, *111*, 8963.
(15) Strohmeier, G. K. *Chem. Ber.* **1961**, *94*, 398.
(16) Hatchard, C. G.; Parker, C. A. *Proc. R. Soc. London, Ser. A* **1956**, *235*, 518.
(17) Belliveau, T. F. Ph.D. Thesis, McGill University, 1988.
(18) Marquardt, D. W. *J. Soc. Ind. Appl. Math.* **1963**, *11*, 431.

0020-1669/91/1330-0567$02.50/0

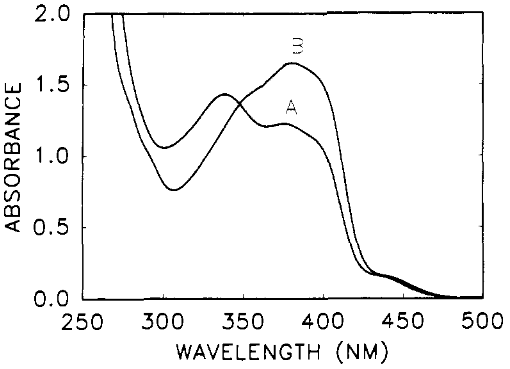

Figure 1. Electronic spectra of W(CO)$_5$py in (A) dichloromethane/1-hexene (2:1) and (B) isooctane/1-hexene (2:1). Concentrations are 2.8 × 10^{-4} M.

Table I. Band Maxima for Transitions in W(CO)$_5$L Determined from Deconvolution of Spectral Bands

	band maxima, nm (±2 nm)						
	W(CO)$_5$py				W(CO)$_5$pip		
solvent	W → py CT	^{1}A	^{1}E	^{3}E	^{1}A	^{1}E	^{3}E
isooctane	352	388	404	448	388	410	448
isooctane/1-hexene	352	388	404	448	388	409	448
1-hexene	354	386	405	448	388	409	448
CCl$_4$/1-hexene	354	386	405	446	389	410	448
C$_6$H$_6$/1-hexene	344	382	402	446	385	408	440
CHCl$_3$/1-hexene	336	384	404	440	389	407	448
CH$_2$Cl$_2$/1-hexene	336	380	400	440	386	406	444

[a] Mixed solvents are in 2:1 ratio with 1-hexene.

Results

Electronic Spectra. The electronic spectra of W(CO)$_5$py and W(CO)$_5$pip exhibit similar features in alkane solvents. In isooctane, each compound exhibits a low-energy band, near 22 625 cm^{-1} (442 nm), which has been previously assigned as a LF $^1A_1 \rightarrow {}^3E$ transition and which appears as a shoulder on the more intense LF ^1E transition centered near 26 180 cm^{-1} (382 nm) for pyridine and 24 350 cm^{-1} (404 nm) for piperidine.[19,20] Higher energy transitions have not been definitively assigned. The symmetry of the band observed for piperidine at ~26 180 cm^{-1} (382 nm) suggests the presence of a second band. On the basis of the splitting of the $^1T_{1g}$ state on reduction from octahedral to C_{4v} symmetry and similar assignments for Rh complexes,[21] this asymmetry is assigned as a contribution from the orbitally forbidden, equatorially directed $^1A \rightarrow {}^1A_2$ transition. The intense absorption at 36 040 cm^{-1} (270 nm) observed for both complexes, by analogy to the MLCT assignment for W(CO)$_6$, is assigned the W → π^* CO CT transition.[22] For W(CO)$_5$py in polar solvents (benzene, dichloromethane, alcohols), the asymmetry of the band observed near 28 570 cm^{-1} (350 nm) in nonpolar solvents (cyclohexane, isooctane, carbon tetrachloride) splits to reveal an absorption band that blue-shifts and is revolved from the LF singlet bands in more polar media (Figure 1). This band has been assigned as a W → pyridine CT transition.[23] Resolution of the CT and LF bands in the pyridine complex in polar solvents reveals another transition at ~370 nm indicated by the asymmetry of the LF band. The assignments based on the Gaussian resolution are collected in Table I.

Photochemistry. 1-Hexene was used as the entering ligand in all solvents studied. Irradiation of both complexes in all solvents leads to efficient replacement of L by 1-Hexene (Figure 2). Irradiation at 436 nm leads to complete conversion with no secondary photolysis for all solvents except CCl$_4$. For CCl$_4$, the appearance of a blue precipitate occurs after approximately 85% conversion. Secondary photolysis leading to the appearance of a white precipitate and subsequent loss of the isosbestic point occurs at greater than 40% conversion under 313-nm irradiation of W(CO)$_5$py and greater than 85% conversion under 365-nm irradiation for both complexes in all solvents. The appearance of the precipitate is not influenced by the presence or absence of oxygen. The precipitate is probably a polymer of 1-hexene produced by W(CO)$_5$L catalysis. Removal of the precipitate restores the isosbestic point. Quantum yields for 313-, 365-, and 436-nm irradiation of both complexes along with five solvent parameters are reported in Table II. The limitation to 10% conversion for

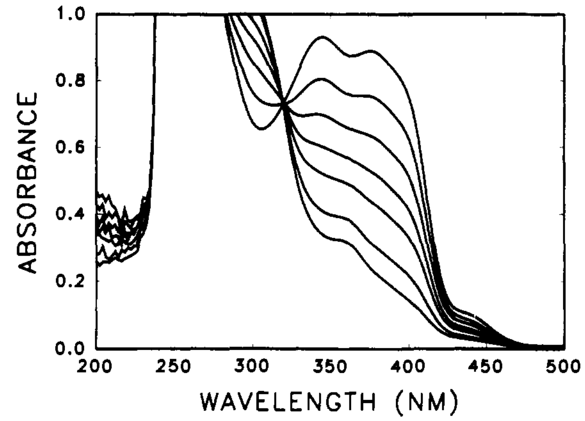

Figure 2. Electronic spectral changes for W(CO)$_5$py in chloroform/1-hexene (2:1 v/v) under 436-nm irradiation. The times of irradiation in order of decreasing absorbance at 380 nm are 0, 30, 60, 90, 120, 180, and 240 s.

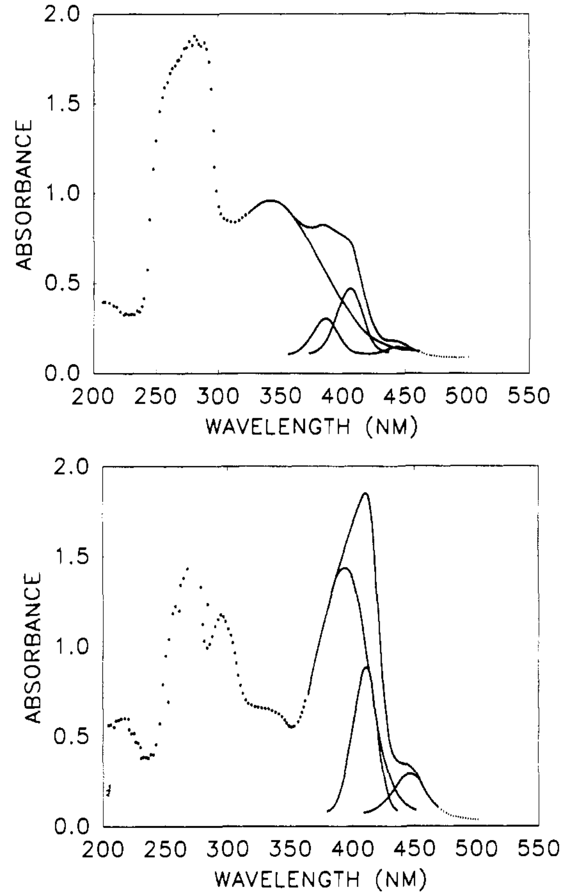

Figure 3. Deconvoluted spectral bands of (a, top) W(CO)$_5$py and (b, bottom) W(CO)$_5$pip in dichloromethane/1-hexene (2:1 v/v).

---

(19) Wrighton, M.; Hammond, G. S.; Gray, H. B. *Inorg. Chem.* **1972**, *11*, 3122.

(20) Wrighton, M.; Pope, K. R. *Inorg. Chem.* **1985**, *24*, 2792.

(21) Miskowski, V. M.; Gray, H. B. *Inorg. Chem.* **1975**, *14*, 401.

(22) Beach, N. A.; Gray, H. B. *J. Am. Chem. Soc.* **1968**, *90*, 5713.

(23) Wrighton, M.; Abramson, G. S.; Gray, H. B. *J. Am. Chem. Soc.* **1976**, *98*, 4105.

(24) Gutmann, V. *Electrochim. Acta* **1976**, *21*, 661.

(25) Reichardt, C. *Angew. Chem., Int. Ed. Engl.* **1979**, *18*, 98.

Table II. Solvent Dependence of Quantum Yields^{a}

						quantum yield				
	solvent parameters^{b}					$W(CO)_5pip$		$W(CO)_5py$		
solvent	AN	ϵ	E_T	Vis	SMW	365 nm	436 nm	313 nm	365 nm	436 nm
CCl_4/1-hexene	2.24	8.6	32.5	0.969	153.82	0.68 (0.02)^{6}	0.55 (0.02)^{14}	0.61 (0.01)^{5}	0.80 (0.02)^{6}	0.74 (0.02)^{12}
1-hexene	2.04				84.16	0.52 (0.03)^{8}	0.62 (0.02)^{12}		0.60 (0.03)^{9}	0.73 (0.03)^{10}
isooctane/1-hexene	1.94		32.0	0.390	114.23	0.49 (0.03)^{15}	0.54 (0.02)^{7}	0.50 (0.03)^{7}	0.53 (0.02)^{15}	0.62 (0.03)^{13}
$CHCl_3$/1-hexene	4.81	23.1	39.1	0.855	119.38	0.45 (0.03)^{5}	0.50 (0.04)^{17}	0.48 (0.02)^{5}	0.47 (0.06)^{8}	0.57 (0.03)^{11}
C_6H_6/1-hexene	2.28	8.2	34.5	0.912	78.11	0.42 (0.02)^{4}	0.45 (0.02)^{11}	0.49 (0.04)^{4}	0.52 (0.02)^{8}	0.55 (0.03)^{6}
CH_2Cl_2/1-hexene	9.08	20.4	41.1	0.450	84.93	0.41 (0.02)^{8}	0.42 (0.02)^{11}	0.38 (0.05)^{13}	0.44 (0.04)^{3}	0.54 (0.01)^{4}

[a] Solvents are mixed in a 2:1 v/v ratio with 1-hexene. Standard deviations are given in parentheses. [b] AN = acceptor number,[24] ϵ = dielectric constant, E_T = local polarity,[25] Vis = viscosity, and SMW = solvent molecular weight. ϵ, Vis, and SMW values were taken from: *Handbook of Chemistry and Physics*, 64th ed.; CRC Press: Boca Raton, FL, 1984.

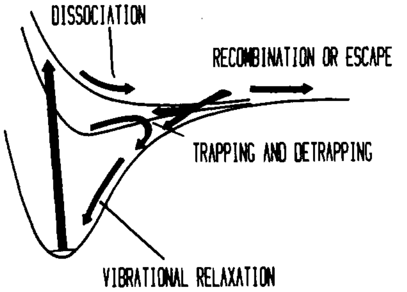

Figure 4. Pictorial representation of photodissociation and recombination processes that occur in solution. Frank–Condon absorption is represented by the vertical arrow.

quantum yield calculation avoids all difficulties with secondary photolysis.

Spectral Assignments. On the basis of the electronic spectral assignments, the curve-fitting program previously described was used to deconvolute the bands in the 300–500- and 350–500-nm regions of the electronic spectra of $W(CO)_5py$ and $W(CO)_5pip$, respectively. Four bands were assigned for $W(CO)_5py$, and three bands, for $W(CO)_5pip$. For $W(CO)_5py$, these four bands represent, in order of increasing energy, transitions to the ^3E, ^1E, ^1A, and MLCT states, respectively. For $W(CO)_5pip$, the three bands represent, in order of increasing energy, transitions to the ^3E, ^1E, and ^1A states, respectively. Examples are shown in Figure 3. If we use the deconvoluted spectra as a guide for $W(CO)_5py$, 313-nm irradiation may initially populate the MLCT state in solvents where the MLCT and LF states are separated. In solvents where the MLCT and LF states overlap, both 313- and 365-nm irradiations populate a mixture of ^1A and MLCT states. An MLCT state does not complicate matters in $W(CO)_5pip$ as it does in $W(CO)_5py$. For $W(CO)_5pip$, 365-nm irradiation initially populates the ^1A component. For both complexes, 436-nm irradiation initially populates mainly the ^1E state with a small contribution from the ^3E state.

Reaction Pathways in $W(CO)_5pip$. In $W(CO)_5pip$, substitution of the unique ligand upon excitation into ^1A can be explained by efficient internal conversion to the reactive ^1E state in competition with efficient relaxation to the ground state. The 436-nm irradiation populates the ^1E state directly, accounting for the higher yields. Competition between radiationless decay and intersystem crossing to the ^3E state can account for yields that are less than unity upon irradiation into the ^1E state. A decreased rate of radiationless decay and/or an increased rate of crossing between states that is dependent on the solvent can account for the trend of increased quantum yields from CH_2Cl_2 to CCl_4. An increased rate of intersystem crossing from ^1E to ^3E may account for yields that are lower upon 436-nm irradiation than upon 365-nm irradiation as is observed for these complexes in CCl_4.

Reaction Pathways in $W(CO)_5py$. The presence of the MLCT state in $W(CO)_5py$, if reaction originated from the CT state, might account for the higher yields observed for this complex than for $W(CO)_5pip$. In CH_2Cl_3, $CHCl_3$, and C_6H_6, the CT and LF states are separated. The 313-nm irradiation of $W(CO)_5py$ gives yields that are comparable to yields for $W(CO)_5pip$. No preferential population of ^1E seems to arise from MLCT excitation, and internal conversion follows a sequence similar to that for $W(CO)_5pip$. In solvents where MLCT and LF states mix, population of ^1E from "CT" absorption is facile; note that the MLCT state has E but not A symmetry. Thus, we believe the presence of CT absorption plays little role in the photochemistry because conversion to LF states is quite facile.

Discussion

Role of the Solvent. Efforts were made to correlate reaction with solvent parameters given in Table II. None of the conventional solvent parameters (viscosity, dielectric constant, local polarity (E_T), and donor number) provide an insight. We must conclude that neither bulk solvent effects nor ligand nucleophilicity can explain yield variations. It is reasonable that the conventional approaches fail. Wavelength-dependent[6] and picosecond-time-resolved[6] studies emphasize that $W(CO)_5L$ species react on time scales too short for full equilibration of the solvent environment. What is clear is that solvent effects must be discussed in terms of their role in mediating internal conversion and intersystem crossing ($^1A \rightarrow {}^1E$ and $^1E \rightarrow {}^3E$) in competition with relaxation to the ground state. The high quantum yields are to be associated with slow relaxation to the ground state (except in the extreme that slow relaxation to the ground state favors intersystem crossing to the less reactive ^3E). It must be added that recombination of the primary photoproducts is one possible pathway for return to the ground state that cannot be distinguished from conventional nonchemical radiationless decay. Figure 4 summarizes the competing pathways.

Two possible mechanisms for efficient radiationless decay must be considered: vibrational–vibrational (VV) and vibrational–translational (VT) energy transfer between the excited solute and solvent molecules. Since competition between radiationless decay and reaction is determined in the critical region Figure 4, high on the potential surface where the vibrational states are spaced closely together, VV energy transfer is less likely to discriminate among solvents and VT energy transfer becomes more important. In our solvent studies, the increase in the quantum yields roughly parallels the increase in masses of the solvents. The highest quantum yield is observed in CCl_4, while the lowest quantum yield is observed in CH_2Cl_2. This suggests that collisions with the massive CCl_4 molecules leads to inefficient energy transfer. This prolongs the excited state and allows for greater internal conversion between the ^1A and the ^1E states and greater intersystem crossing between the ^1E and ^3E states. This can explain the highest yields observed upon 365-nm irradiation in CCl_4 as the rate of radiationless decay decreases and the rate of internal conversion from the less reactive ^1A state to the more reactive ^1E state increases. This line of analysis appears to be the only approach capable of explaining the unique decrease in quantum yield from 365 to 436 nm in CCl_4. The slow radiationless decay has allowed an increase in intersystem crossing to the ^3E state, which is less reactive.

Acknowledgment. We thank the Natural Sciences and Engineering Research Council of Canada for support of this work and a fellowship to C.M. The work also benefitted from the Actions Structurantes Program of the Ministere d'Enseignement Superieur et de la Science du Quebec.